

Accepted Manuscript

Vertical vibration of a rigid circular disc at the interface of a transversely isotropic bi-material

A.R. Hajimohammadi, A. Khojasteh, M. Rahimian, R.Y. S.Pak

PII: S0020-7683(13)00181-9

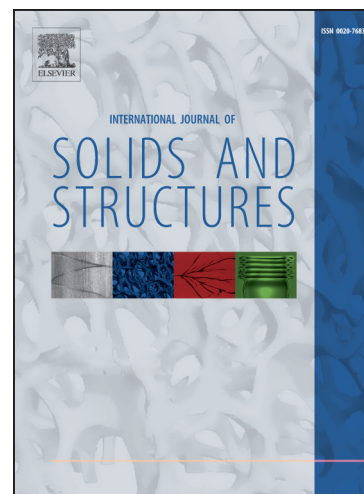
DOI: <http://dx.doi.org/10.1016/j.ijsolstr.2013.04.024>

Reference: SAS 7984

To appear in: *International Journal of Solids and Structures*

Received Date: 25 November 2012

Revised Date: 25 March 2013



Please cite this article as: Hajimohammadi, A.R., Khojasteh, A., Rahimian, M., S.Pak, R.Y., Vertical vibration of a rigid circular disc at the interface of a transversely isotropic bi-material, *International Journal of Solids and Structures* (2013), doi: <http://dx.doi.org/10.1016/j.ijsolstr.2013.04.024>

This is a PDF file of an unedited manuscript that has been accepted for publication. As a service to our customers we are providing this early version of the manuscript. The manuscript will undergo copyediting, typesetting, and review of the resulting proof before it is published in its final form. Please note that during the production process errors may be discovered which could affect the content, and all legal disclaimers that apply to the journal pertain.

Vertical vibration of a rigid circular disc at the interface
of a transversely isotropic bi-material

A. R. Hajimohammadi

School of Civil Engineering
College of Engineering
University of Tehran
P.O. Box 11155-4563
Iran

A. Khojasteh

Department of Engineering Science
College of Engineering
University of Tehran
P.O. Box 11155-4563
Iran

E-mail address: akhojasteh@ut.ac.ir

M. Rahimian¹

School of Civil Engineering
College of Engineering
University of Tehran
P.O. Box 11155-4563
Iran

E-mail address: rahimian@ut.ac.ir

Tel.: +98 21 61112256

Fax: +98 21 88078263

R.Y.S. Pak

Department of Civil, Environmental and Architectural Engineering
University of Colorado
Boulder, CO 80309-0428,
U.S.A.

E-mail address: pak@colorado.edu

¹Corresponding author

Vertical vibration of a rigid circular disc at the interface of a transversely isotropic bi-material

A.R. Hajimohammadi, A. Khojasteh, M. Rahimian, R. Y. S. Pak

ABSTRACT

A theoretical formulation is presented for the determination of the dynamic interaction of a vertically loaded rigid disc embedded at the interface of a transversely isotropic bi-material full-space. With the aid of Hankel integral transforms, a relaxed treatment of the mixed-boundary value problem is formulated as dual integral equations, which can be reduced to a Fredholm integral equation of the second kind. The dynamic contact pressure under the disc and the impedance function are analytically evaluated in the general dynamic case. It is shown that the impedance functions are in exact agreement with the existing solutions for an elastic half-space with isotropic material properties. To confirm the accuracy of the numerical evaluation of the integrals involved, numerical results are included for cases of different degrees of the material anisotropy and compared with previously published solutions.

Keywords: Transversely isotropic, Bi-material, Green's function, Rigid disc, Dual integral equations, Impedance function

1. INTRODUCTION

The increased use of composite materials in engineering applications in recent decades has become an incentive for extensive research, both basic and applied, into various failure modes of such materials. It was also recognized that the performance of composite materials was closely related to the effects occurring at the interface between the different components of the composite. Issues such as interfacial fracture and crack problems in bi-material systems are at the forefront of many investigations (Lambros and Rosakis, 1995). The reader is referred to Prasad et al. (2005) and Wu et al. (2003) for an extensive list of work in this area. In the field of geomechanics and foundation engineering, a thin embedded inclusion can serve as a basic model for an anchoring region, which can be created by the injection of a cementitious material (Selvadurai, 1994). The evaluation of the elastic stiffness of these embedded anchoring devices is of particular interest to predict the failure at either the interface or adjacent regions (Selvadurai, 2003). The introduction of the cementitious material under pressure can lead to hydraulic fracturing of the material in a plane normal to the least principal

value of the geostatic stresses and the migration of the cementitious fluid within the narrow fracture invariably leads to a disc shaped anchoring region. Also the migration pattern of the viscous cementitious fluid within the fracture is a complex problem in itself. Often, the flat anchoring region will have an irregular shape that is largely determined by local inhomogeneities at the plane of the fracture. (Selvadurai, 2003, 2000). As an idealized model of the anchoring region, Selvadurai (2003) studied the mechanics of a loaded rigid disc that is embedded in bonded contact at the interface between two dissimilar isotropic elastic media. The dynamic interaction of a rigid disc with an isotropic media, has also been studied (Gladwell, 1968; Luco and Mita, 1987; Pak and Gobert, 1991; Reissner and Sagoci, 1944; Robertson, 1966).

For many modern technological applications, however, the isotropic material model can sometimes be only a crude approximation. Numerous innovative, smart, and intelligent materials, such as composites, piezomagnetism and piezoelectrics, are anisotropic and in application should be modeled at least as an transversely isotropic or orthotropic material. Katebi et al. (2010) have made an in-depth investigation for the analytical solution of an axially symmetric interaction of a rigid disc with a homogenous transversely isotropic half-space in the static case. Also, Moghaddasi et al. (2012) solved the dual integral equations due to horizontal interaction of a rigid circular disc in a transversely isotropic half-space (also see, e.g. Kirkner, 1982; Pak and Gobert, 1990; Rahman, 2001; Shahmohamadi et al., 2012, 2011a, 2011b; Zeng and Rajapakse, 1999). In this paper, the vertical vibration of a rigid circular disc located at the interface of a transversely isotropic bi-material full-space is considered. Employing the Green's functions of a transversely isotropic bi-material full-space introduced by Khojasteh et al. (2008), the mixed boundary-value problem is transformed to a pair of integral equations, called Fredholm dual integral equations. In the different's cases of dual integral equations, it can be referred to different researchers (Mandal and Mandal, 1999; Noble, 1963; Sneddon, 1966). The general solution for the Fredholm integral equation is numerically determined, and the dynamic vertical pressure under the disc, and the impedance function, are numerically evaluated. The impedance/compliance function for an isotropic full-space is degenerated from the present solutions and are identical to the solutions given by Luco and Mita (1987) and Pak and Gobert (1991) for any frequency. To show the effect of different material anisotropy and frequency of vibration, on the response selected numerical results are also given.

2. STATEMENT OF THE PROBLEM AND THE GOVERNING EQUATIONS

With reference to Fig. 1, consider a rigid disc of radius a , embedded at an interface of a transversely isotropic, elastic bi-material full-space. The disc is assumed to be undergoing a prescribed time-harmonic vertical displacement, $\Delta e^{i\omega t}$, with Δ and ω being the amplitude and circular frequency of the motion,

respectively. In view of the axial symmetry of the problem, it is natural to adopt the cylindrical coordinates (r, θ, z) , so that the angular dependence of the solution can be suppressed. A relaxed treatment of this mixed boundary-value problem can be stated in terms of the components of the displacement vector u and the Cauchy stress tensor σ as follows:

$$u_z(r, z=0) = \Delta \quad r \leq a \quad (1)$$

$$u_z(r, z=0^-) - u_z(r, z=0^+) = 0 \quad r \geq 0 \quad (2)$$

$$u_r(r, z=0^-) - u_r(r, z=0^+) = 0 \quad r \geq 0 \quad (3)$$

$$u_\theta(r, z) = 0 \quad r \geq 0, z \in (-\infty, +\infty) \quad (4)$$

$$\sigma_{rz}(r, z=0^-) - \sigma_{rz}(r, z=0^+) = 0 \quad r \geq 0 \quad (5)$$

$$\sigma_{zz}(r, z=0^-) - \sigma_{zz}(r, z=0^+) = R(r) \quad r \leq a \quad (6)$$

$$\sigma_{zz}(r, z=0^-) - \sigma_{zz}(r, z=0^+) = 0 \quad r > a \quad (7)$$

Here, $R(r)$ represents the unknown net load distribution acting on the disc. The equations of time-harmonic motion for a homogeneous transversely isotropic elastic solid in terms of displacements and in the absence of body forces can be expressed as (Lekhnitskii, 1981)

$$C_{11} \left(\frac{\partial^2 u_r}{\partial r^2} + \frac{1}{r} \frac{\partial u_r}{\partial r} - \frac{u_r}{r^2} \right) + C_{44} \frac{\partial^2 u_r}{\partial z^2} + (C_{13} + C_{44}) \frac{\partial^2 u_r}{\partial r \partial z} + \rho \omega^2 u_r = 0 \quad (8)$$

$$C_{44} \left(\frac{\partial^2 u_z}{\partial r^2} + \frac{1}{r} \frac{\partial u_z}{\partial r} \right) + C_{33} \frac{\partial^2 u_z}{\partial z^2} + (C_{13} + C_{44}) \left(\frac{\partial^2 u_r}{\partial r \partial z} + \frac{1}{r} \frac{\partial u_r}{\partial z} \right) + \rho \omega^2 u_z = 0 \quad (9)$$

in a cylindrical coordinate system (r, θ, z) , where z -axis is the axis of symmetry of the solid; u_r and u_z are the displacement components in the r and z directions, respectively; ρ is the mass density of the solid; c_{ij} is the elasticity constants of the solid; and the time factor $e^{i\omega t}$ is suppressed. In order to uncouple Eqs. (8) and (9), a potential function F , introduced by Eskandari-Ghadi (2005), is used. Using the potential function F and interfacial traction conditions, together with the displacement conditions across the interface, provides the equations required for the solutions for u_r and u_z in terms of the transformed Fourier component of the contact-load distribution z_m (Khojasteh et al., 2008). In particular, one may verify that the radial and vertical displacements can in general be expressed as (Khojasteh et al., 2008)

$$u_{zm} = \int_0^\infty \xi \{ \Omega_2(\xi, z) \left(\frac{z_m}{c_{44}} \right) \} J_m(r\xi) d\xi \quad (10)$$

$$u_{rm} = \int_0^\infty \xi \{ -\gamma_3(\xi, z) \left(\frac{z_m}{c_{44}} \right) \} J_{m+1}(r\xi) d\xi \quad (11)$$

In the above

$$\gamma_3(\xi, z) = \frac{-\alpha_3 c_{44} \xi}{S(\xi)} \frac{z}{|z|} (\lambda_1 \kappa_2 e^{-\lambda_1 |z|} - \lambda_2 \kappa_1 e^{-\lambda_2 |z|}) \quad (12)$$

$$\Omega_2(\xi, z) = \frac{-c_{44}}{S(\xi)} (\vartheta_1 \kappa_2 e^{-\lambda_1 |z|} - \vartheta_2 \kappa_1 e^{-\lambda_2 |z|}) \quad (13)$$

and λ_1 and λ_2 are made single-valued by specifying the branch cuts emanating from the branch points $\xi_{\lambda_1} = \omega\sqrt{\rho/c_{11}}$ and $\xi_{\lambda_2} = \omega\sqrt{\rho/c_{44}}$ on the complex ξ -plane (see Fig. 2) such that the real parts of λ_1 and λ_2 are always non-negative (Khojasteh et al., 2008). Here

$$Z_0(\xi) = \tilde{R}^0(\xi) \quad (14)$$

$$\vartheta_i = \alpha_3 \lambda_i^2 - \eta_i \quad (15)$$

$$\eta_i = (\alpha_3 - \alpha_2) \lambda_i^2 + (1 + \alpha_1) \xi^2 - \frac{\rho \omega^2}{c_{66}} \quad (16)$$

$$v_i = c_{33} \left(\eta_i - \alpha_3 \frac{c_{13}}{c_{33}} \xi^2 - \alpha_3 \lambda_i^2 \right) \lambda_i \quad (i = 1, 2) \quad (17)$$

$$\lambda_1 = \sqrt{a \xi^2 + b + \frac{1}{2} \sqrt{c \xi^4 + d \xi^2 + e}} \quad (18)$$

$$\lambda_2 = \sqrt{a \xi^2 + b - \frac{1}{2} \sqrt{c \xi^4 + d \xi^2 + e}}$$

$$a = \frac{1}{2} (s_1^2 + s_2^2), \quad b = -\frac{1}{2} \rho \omega^2 \left(\frac{1}{c_{33}} + \frac{1}{c_{44}} \right), \quad c = (s_2^2 - s_1^2)^2 \quad (19)$$

$$d = -2 \rho \omega^2 \left[\left(\frac{1}{c_{33}} + \frac{1}{c_{44}} \right) (s_1^2 + s_2^2) - 2 \frac{c_{11}}{c_{33}} \left(\frac{1}{c_{11}} + \frac{1}{c_{44}} \right) \right], \quad e = \rho^2 \omega^4 \left(\frac{1}{c_{33}} - \frac{1}{c_{44}} \right)$$

Here, s_1 and s_2 are the roots of following equation, which in view of the positive-definiteness of the strain energy are not zero or pure imaginary numbers (Lekhnitskii, 1981):

$$c_{33} c_{44} s^4 + (c_{13}^2 + 2 c_{33} c_{44} - c_{11} c_{33}) s^2 + c_{11} c_{44} = 0 \quad (20)$$

In expressions (10) – (20), c_{kl} and ρ are the piecewise constant elastic moduli and density, respectively; given by

$$c_{kl} = \begin{cases} c_{kl}^I, & z < 0 \\ c_{kl}^{II}, & z > 0 \end{cases}, \quad \rho = \begin{cases} \rho^I, & z < 0 \\ \rho^{II}, & z > 0 \end{cases} \quad (21)$$

Subsequently, the same expressions are valid for α_i , λ_i , η_i , v_i and ϑ_i . In addition, κ_i is function defined as

$$\kappa_i = \alpha_3^I c_{44}^{II} (\vartheta_1^{II} \eta_2^{II} - \vartheta_2^{II} \eta_1^{II}) \lambda_i^I + \alpha_3^{II} [c_{44}^I (\vartheta_1^{II} \lambda_2^{II} - \vartheta_2^{II} \lambda_1^{II}) \eta_i^I - c_{44}^{II} (\eta_1^{II} \lambda_2^{II} - \eta_2^{II} \lambda_1^{II}) \vartheta_i^I], \quad i = 1, 2 \quad (22)$$

in the upper medium, and

$$\kappa_i = \alpha_3^{II} c_{44}^I (\vartheta_1^I \eta_2^I - \vartheta_2^I \eta_1^I) \lambda_i^{II} + \alpha_3^I [c_{44}^{II} (\vartheta_1^I \lambda_2^I - \vartheta_2^I \lambda_1^I) \eta_i^{II} - c_{44}^I (\eta_1^I \lambda_2^I - \eta_2^I \lambda_1^I) \vartheta_i^{II}], \quad i = 1, 2 \quad (23)$$

in the lower medium. Also

$$S(\xi) = \alpha_3^{\text{II}} [c_{44}^{\text{II}} (\vartheta_1^{\text{I}} v_2^{\text{I}} - \vartheta_2^{\text{I}} v_1^{\text{I}}) (\eta_1^{\text{II}} \lambda_2^{\text{II}} - \eta_2^{\text{II}} \lambda_1^{\text{II}}) - c_{44}^{\text{I}} (\eta_1^{\text{I}} v_2^{\text{I}} - \eta_2^{\text{I}} v_1^{\text{I}}) (\vartheta_1^{\text{II}} \lambda_2^{\text{II}} - \vartheta_2^{\text{II}} \lambda_1^{\text{II}}) + c_{44}^{\text{I}} (\vartheta_1^{\text{I}} \eta_2^{\text{I}} - \vartheta_2^{\text{I}} \eta_1^{\text{I}}) (v_1^{\text{II}} \lambda_2^{\text{II}} - v_2^{\text{II}} \lambda_1^{\text{II}})] \\ + \alpha_3^{\text{I}} [c_{44}^{\text{I}} (\vartheta_1^{\text{II}} v_2^{\text{II}} - \vartheta_2^{\text{II}} v_1^{\text{II}}) (\eta_1^{\text{I}} \lambda_2^{\text{I}} - \eta_2^{\text{I}} \lambda_1^{\text{I}}) - c_{44}^{\text{II}} (\eta_1^{\text{II}} v_2^{\text{II}} - \eta_2^{\text{II}} v_1^{\text{II}}) (\vartheta_1^{\text{I}} \lambda_2^{\text{I}} - \vartheta_2^{\text{I}} \lambda_1^{\text{I}}) + c_{44}^{\text{II}} (\vartheta_1^{\text{II}} \eta_2^{\text{II}} - \vartheta_2^{\text{II}} \eta_1^{\text{II}}) (v_1^{\text{I}} \lambda_2^{\text{I}} - v_2^{\text{I}} \lambda_1^{\text{I}})] \quad (24)$$

is associated Stoneley wave function. In the case of an isotropic material Eq. (25) reduces to the following expression

$$\left(\frac{\lambda^{\text{I}} + \mu^{\text{I}}}{\mu^{\text{I}}} \right)^2 \left(\frac{\lambda^{\text{II}} + \mu^{\text{II}}}{\mu^{\text{II}}} \right)^2 \alpha^{\text{I}} \alpha^{\text{II}} S^{\text{iso}}(\xi) \quad (25)$$

where

$$S^{\text{iso}}(\xi) = -\{4\xi^2(\mu^{\text{II}} - \mu^{\text{I}})^2(\xi^2 - \alpha^{\text{I}}\beta^{\text{I}})(\xi^2 - \alpha^{\text{II}}\beta^{\text{II}}) + 4\xi^2\omega^2(\mu^{\text{II}} - \mu^{\text{I}})[\rho^{\text{I}}(\xi^2 - \alpha^{\text{II}}\beta^{\text{II}}) - \rho^{\text{II}}(\xi^2 - \alpha^{\text{I}}\beta^{\text{I}})] \\ + \xi^2\omega^4(\rho^{\text{II}} - \rho^{\text{I}})^2 - \omega^4(\rho^{\text{I}}\beta^{\text{II}} + \rho^{\text{II}}\beta^{\text{I}})(\rho^{\text{I}}\alpha^{\text{II}} + \rho^{\text{II}}\alpha^{\text{I}})\} \quad (26)$$

Again in the above expressions, superscripts I and II denote the quantities in media I and II, respectively; λ and μ are Lamé constants of elasticity; $\alpha = \sqrt{\xi^2 - \rho\omega^2/(\lambda + 2\mu)}$ and $\beta = \sqrt{\xi^2 - \rho\omega^2/\mu}$. Eq. (26) degenerates exactly to the expression given in Pak and Guzina (2002) for the Stoneley wave function corresponding to the interface between two adjacent isotropic layers. On substituting the inverted Fourier components of the displacements and stresses into the corresponding angular eigenfunction expansions, the desired formal solution to the general bi-material problem under consideration can be obtained. With the aid of the relations (10) and (14), it can be shown that the remaining two conditions (1) and (7) of the mixed boundary-value problem are equivalent to

$$\int_0^\infty \Omega_2(\xi, z) \frac{\xi Z_0(\xi)}{c_{44}} J_0(r\xi) d\xi = \Delta \quad r \leq a \quad (27)$$

and

$$\int_0^\infty Z_0(\xi) \xi J_0(r\xi) d\xi = 0 \quad r > a \quad (28)$$

which are a pair of dual integral equations. By setting $z = 0$ for the surface disc in the integrand of (27) and (28), the formulation degenerates to

$$\int_0^\infty \Omega_2(\xi, z = 0) \frac{\xi Z_0(\xi)}{c_{44}} J_0(r\xi) d\xi = \Delta \quad r \leq a \quad (29)$$

and

$$\int_0^\infty Z_0(\xi) \xi J_0(r\xi) d\xi = 0 \quad r > a \quad (30)$$

where

$$\Omega_2(\xi, z=0) = \frac{-c_{44}}{S(\xi)} (\vartheta_1 \kappa_2 - \vartheta_2 \kappa_1) \quad (31)$$

Equation (31) has the properties that

$$\lim_{\xi \rightarrow +\infty} \xi \Omega_2(\xi, z=0) = L^{-1} \quad (32)$$

In the upper limit, L is a modifier for this function to make the condition at infinity to be satisfied and both sides of the first equation in dual integral equations should be divided by this modifier. The quantities of L in the general dynamic case are a function of combination of different full-space properties.

3. REDUCTION OF SYSTEM OF DUAL INTEGRAL EQUATIONS

For the treatment of the dual integral Equations (29, 30) in the general problem, it is convenient to re-write them as:

$$\int_0^\infty \frac{1}{\xi} [1 + H(\xi; \omega)] B(\xi; \omega) J_0(r\xi) d\xi = \delta_s \quad r \leq a \quad (33)$$

and

$$\int_0^\infty B(\xi; \omega) J_0(r\xi) d\xi = 0 \quad r > a \quad (34)$$

where

$$B(\xi; \omega) = \frac{\xi Z_0(\xi)}{c_{44}} \quad (35)$$

$$H(\xi; \omega) = L\Omega_2(\xi, z)\xi - 1, \quad \delta_s = \Delta \cdot L \quad (36)$$

With the aid of Sonine's integrals (Noble, 1963), one can show that the integrals (33) and (34) is transformed to

$$\int_0^\infty \xi^{-\frac{1}{2}} [1 + H(\xi; \omega)] B(\xi; \omega) J_{-1/2}(r\xi) d\xi = \frac{r^{-1/2}}{2^{-1/2} \Gamma(\frac{1}{2})} \delta_s \quad r \leq a \quad (37)$$

and

$$\int_0^\infty \xi^{-1/2} B(\xi; \omega) J_{-1/2}(r\xi) d\xi = 0 \quad r > a \quad (38)$$

In (37), $\Gamma(x)$ is the Gamma function. For further reduction, it is useful to define a function θ through

$$B(\xi; \omega) = \frac{\xi^{3/2}}{2^{-1/2} \Gamma(\frac{1}{2})} \int_0^a \varrho^{1/2} \theta(\varrho; \omega) J_{-1/2}(\varrho \xi) d\varrho \quad \xi \in [0, \infty) \quad (39)$$

which, on inversion, gives

$$\theta(r; \omega) = \begin{cases} \frac{r^{1/2} \Gamma(\frac{1}{2})}{2^{1/2}} \int_0^\infty \xi^{-1/2} B(\xi; \omega) J_{-1/2}(r\xi) d\xi & 0 \leq r < a \\ 0 & r > a \end{cases} \quad (40)$$

With the aid of (39) and (40), the dual integral equations in (37) and (38) can be reduced to a Fredholm integral equation of the second kind

$$\theta(r; \omega) + \int_0^a K(r, \varrho) \theta(\varrho; \omega) d\varrho = \delta_s \quad 0 \leq r < a \quad (41)$$

where

$$K(r, \varrho) = (r\varrho)^{1/2} \int_0^\infty \xi H(\xi; \omega) J_{-1/2}(r\xi) J_{-1/2}(\varrho\xi) d\xi, \quad 0 \leq r < a, \quad 0 \leq \varrho < a \quad (42)$$

Writing $J_{-1/2}(\eta)$ in terms of cosine function as $J_{-1/2}(\eta) = \sqrt{\frac{2}{\pi\eta}} \cos(\eta)$, Eq. (42) can be written as

$$K(r, \varrho) = 2 \int_0^\infty H(\xi; \omega) \cos(r\xi) \cos(\varrho\xi) d\xi, \quad 0 \leq r < a, \quad 0 \leq \varrho < a \quad (43)$$

Eq. (41) with (42) or (43) can be numerically solved for $\theta(r; \omega)$. For numerical purposes, the Fredholm integral Eq. (41) can be converted to a set of linear algebraic equations of the form (Katebi et al., 2009; Moghaddasi et al., 2012; Pak and Gobert, 1990; Pak and Gobert, 1991)

$$M_{ij} \theta_j = f_i \quad i, j = 1, 2, \dots, n \quad (44)$$

where

$$M_{ij} = \delta_{ij} + W_j K(r_i, \varrho_j) \quad i, j = 1, 2, \dots, n \quad (45)$$

$$f_i = \Delta_i L \quad i = 1, 2, \dots, n \quad (46)$$

moreover, W_j is the weight function for transforming an integral to a summation, and n is the number of point selected on the disc for numerical evaluation.

4. Special cases

In this section, it is relevant to examine two degenerate cases: (i) when the moduli of both media are equal, and (ii) when the modulus of the upper medium $z < 0$ is zero. As it is apparent from the physics of the problem, such degenerate forms of the general formulation should correspond to the homogeneous full-space and half-space solutions, respectively.

4.1. Homogeneous transversely isotropic full-space

Upon setting $c_{kl}^I = c_{kl}^{II} = c_{kl}$ and $\rho^{II} = \rho^I = \rho$, the kernel functions (12) and (13) can be reduced to

$$\gamma_3(\xi, z) = \frac{\alpha_3 c_{44} \xi}{2\alpha_2 c_{33}(\lambda_1^2 - \lambda_2^2)} \frac{z}{|z|} (e^{-\lambda_1|z|} - e^{-\lambda_2|z|}) \quad (47)$$

$$\Omega_2(\xi, z) = \frac{c_{44}}{2\alpha_2 c_{33}(\lambda_1^2 - \lambda_2^2)} \left(\frac{\vartheta_1}{\lambda_1} e^{-\lambda_1|z|} - \frac{\vartheta_2}{\lambda_2} e^{-\lambda_2|z|} \right) \quad (48)$$

for the homogeneous full-space problem.

4.2. Homogeneous transversely isotropic half-space

Taking $c_{kl}^I \rightarrow 0, \rho^I \rightarrow 0, c_{kl}^{II} = c_{kl}$ and $\rho^{II} = \rho$, degenerates the kernel functions (12) and (13) to the following expressions for the half-space problem

$$\gamma_3(\xi, z) = \frac{-\alpha_3 c_{44} \xi}{c_{33} I(\xi)} (\eta_2 \lambda_1 e^{-\lambda_1 z} - \eta_1 \lambda_2 e^{-\lambda_2 z}) \quad (49)$$

$$\Omega_2(\xi, z) = \frac{c_{44}(1+\alpha_1)}{c_{33} I(\xi)} \left\{ \left(\xi^2 - \frac{\rho \omega^2}{c_{11}} \right) (\eta_2 e^{-\lambda_1 z} - \eta_1 e^{-\lambda_2 z}) - \frac{\alpha_2}{(1+\alpha_1)} (\eta_2 \lambda_1^2 e^{-\lambda_1|z|} - \eta_1 \lambda_2^2 e^{-\lambda_2 z}) \right\} \quad (50)$$

where

$$I(\xi) = \eta_2 v_1 - \eta_1 v_2 \quad (51)$$

is the Rayleigh wave function whose zero at ξ_R corresponds to the Rayleigh wave number associated with the free surface in the half-space medium. The kernel functions in Eqs. (49-50) are exactly the same as those obtained in Rahimian et al. (2007) for a transversely isotropic half-space under surface excitations.

4.3. Homogeneous isotropic half-space

The material constants for an isotropic medium can be reduced to

$$c_{11} = c_{33} = \lambda + 2\mu, \quad c_{12} = c_{13} = \lambda, \quad c_{44} = c_{66} = \mu \quad (52)$$

where λ and μ are the Lamé's constants of the isotropic solid. and

$$\lambda_1 = \alpha = \sqrt{\xi^2 - k_p^2}, \quad \lambda_2 = \beta = \sqrt{\xi^2 - k_s^2} \quad (53)$$

Using these relations, the kernel functions (12) and (13) can be reduced to

$$\gamma_3(\xi, z) = \frac{\xi}{2k_s^2} (e^{-\alpha z} - e^{-\beta z}) + \frac{\xi}{2k_s^2} \frac{R^+(\xi)}{R^-(\xi)} (e^{-\alpha z} + e^{-\beta z}) - \frac{2\xi(2\xi^2 - k_s^2)}{k_s^2 R^-(\xi)} (\xi^2 e^{-\alpha z} + \alpha\beta e^{-\beta z}) \quad (54)$$

$$\begin{aligned} \Omega_2(\xi, z) = & -\frac{\alpha}{2k_s^2} e^{-\alpha z} + \frac{\xi^2}{2\beta k_s^2} e^{-\beta z} - \frac{1}{2k_s^2} \frac{R^+(\xi)}{R^-(\xi)} \left(\alpha e^{-\alpha z} + \frac{\xi^2}{\beta} e^{-\beta z} \right) \\ & + \frac{2\xi^2 \alpha (2\xi^2 - k_s^2)}{k_s^2 R^-(\xi)} (e^{-\alpha z} + e^{-\beta z}) \end{aligned} \quad (55)$$

where

$$R^\pm(\xi) = (2\xi^2 - k_s^2)^2 \pm 4\xi^2 \alpha\beta \quad (56)$$

The above kernel functions are exactly the same as those presented by Pak and Gobert (1991).

5. RESPONSE OF THE TRANSVERSELY ISOTROPIC BI-MATERIAL FULL-SPACE

As noted in (10) and (14), the vertical displacement field can be expressed as

$$u_z(r, z; \omega) = \int_0^\infty \Omega_2(\xi, z) \frac{\xi \tilde{R}^0(\xi)}{c_{44}} J_0(r\xi) d\xi \quad (57)$$

Correspondingly, with the aid of (11) and (14), it can be shown that the radial displacement field can be written as

$$u_r(r, z; \omega) = \int_0^\infty -\gamma_3(\xi, z) \frac{\xi \tilde{R}^0(\xi)}{c_{44}} J_1(r\xi) d\xi \quad (58)$$

With the aid of (14), (35), (39), and $J_{-1/2}(\eta) = \sqrt{\frac{2}{\pi\eta}} \cos(\eta)$, the transformed contact load distribution can be expressed as

$$\tilde{R}^0(\xi) = \frac{c_{44} B(\xi; \omega)}{\xi} = \frac{2c_{44}}{\pi} \int_0^a \theta(\varrho; \omega) \cos(\xi\varrho) d\varrho \quad (59)$$

The displacement field can be directly obtained in terms of θ by substituting (59) into (57) and (58). Analogous to displacements, stress field can also be obtained as (Khojasteh et al., 2008)

$$\sigma_{zz}(r, z; \omega) = \int_0^\infty \left\{ c_{33} \frac{d\Omega_2}{dz} - c_{13} \xi \gamma_3 \right\} \frac{\xi \bar{R}^0(\xi)}{c_{44}} J_0(r\xi) d\xi \quad (60)$$

The impedance function is defined as

$$K_{zz}(\omega) = F/\Delta \quad (61)$$

where

$$F = 4c_{44}a \int_0^a \theta(q; \omega) dq \quad (62)$$

6. NUMERICAL EVALUATION OF THE FREDHOLM INTEGRAL EQUATION

In Section 3, the Fredholm integral Eq. (40), was expressed in terms of $\theta(q; \omega)$. In general, these integral equations cannot be carried out in exact closed forms, as a result a numerical quadrature technique usually has to be adopted in such evaluations (see, e.g. Apsel and Luco, 1983; Khojasteh et al. 2008; Pak and Gobert, 1991; Pak and Saphores, 1991; Rahimian et al. 2007; Rajapakse and Wang, 1993). For numerical purposes, the equation may be converted to a set of linear algebraic equations in the form of $M_{ij}\theta_j = f_i$, where M_{ij} and f_i are given in (45) and (46). To evaluate $K_{ij} = K(r_i, q_j)$ from the line integral (43), an adaptive numerical quadrature approach is adopted and coded in MATHEMATICA software.

The function $S(\zeta)$ defined in (24) yields a pole at ξ_s which corresponds to the Stoneley wave number. The pole is obtained by setting $S(\zeta) = 0$. Depending on the elasticity constants and mass density of the two bonded half-spaces, a Stoneley wave may or may not exist. When it does exist in the subsonic regime, only one such interfacial wave is possible and it travels at a speed larger than the smaller of the Rayleigh speeds associated with the two half-spaces (Barnett et al., 1985; Barnett, 2000; Destrade and Fu, 2006; Khojasteh et al., 2008). In other words, the Stoneley wave number must be smaller than the larger of the Rayleigh wave numbers associated with the two half-spaces. As a result the path of integration may be free of poles or not. Once the locations of the singular points are determined, the path of integration is deformed by semi-circles of radius ε around them (see Fig. 2).

While the kernel of the inversion integral is weakly singular at the branch points, it is strongly singular at the pole if it exists. Thus, the integral over the limiting small semi-circle at the pole should be evaluated using the residua theory of integration (Churchill and Brown, 1990). Since the pole at ζ_s is an interior singular point of the first order, the integrand may be written in the form of $q(\zeta)/S(\zeta)$, where $q(\zeta)$ is analytic at ζ_s where ζ_s is the root of the equation $S(\zeta) = 0$ (Khojasteh et al., 2008). Therefore the integral over the limiting small semi-circle at the pole is equal to $-\pi i \text{Res}(\zeta_s)$, where $\text{Res}(\zeta_s) = \lim_{\xi \rightarrow \zeta_s} \left[q(\xi) / \left(\frac{dS(\xi)}{d\xi} \right) \right]$. The procedure adopted in this study involves: (1) locating the pole and branch points associated with branch cuts that render all functions single valued and consistent with the regularity condition; (2) integrating from zero to a point behind the pole and continuing the integration from a point after the pole to a sufficiently large value; and (3) adding the contribution from the residue at the pole to the final sum.

In order to validate the present solutions and their accuracy, numerical solutions presented by Luco and Mita (1987) and Pak and Gobert (1991) for the isotropic case are used in the comparison. It needs to be pointed out that all the numerical results presented here are dimensionless, with a nondimensional frequency defined as $\omega_0 = a\omega \sqrt{\frac{\rho_{II}}{c_{44}}}$. To demonstrate the influence of the degree of the material anisotropy a parametric study is conducted. Several synthetic types of isotropic material and transversely isotropic materials are considered to constitute basic materials. The material properties are given in Table 1, where E and E' are the Young's moduli with respect to directions lying in the plane of isotropy and perpendicular to it; ν is the Poisson's ratio which characterizes the effect of horizontal strain on the complementary vertical strain; ν' is the Poisson's ratio which characterizes the effect of vertical strain on the horizontal one; and c_{44} is the shear modulus in the plane normal to the plane of isotropy. The relation of these parameters to the elasticity constants, c_{ij} can be found in Rahimian et al. (2007). Regarding the positive definiteness of the strain energy, the subsequent restrictions for material constants c_{ij} have been checked (Payton, 1983), $c_{11} > |c_{12}|$, $(c_{11} + c_{12})c_{33} > 2c_{13}^2$, $c_{44} > 0$. To determine the vertical impedance function $K_{zz}(\omega)$, one needs to find the vertical resultant force, F , applied from the disc on the bi-material full-space, from Equation (62). Then, the vertical impedance function is found from (61). The Case of Mat q – Mat q' is used to denote a bi-material full-space consists of an upper half-space contains of Material q and a lower half-space contains of Material q' . To provide a glimpse of the influence of the compressibility of the medium on the contact load distribution, two plots of $R(r)$ for different transversely isotropic materials and dimensionless frequencies $\omega_0 = 0.5$ and 3 are shown in Figs. 3 and 4. From the illustration, it is apparent that the contact load distribution tends to become more accentuated at the edge of the

disc as E'/E and G'/G increases when other engineering properties are kept constant. The influences of the degree of the material anisotropy on vertical variations of σ_{zz} are illustrated in Figs. 5 and 6 for $\omega_0 = 0.5$ and 3. Note that in the determination of σ_{zz} the engineering constant E' is the dominant component, and since its value for the material I is the largest, the value of $\text{Re}(\sigma_{zz})$ in this material is the highest for different bimetals at constant delta. Figs. 7 and 8 show the vertical displacement at $z = 0$ in terms of radial distance, and at $r = 0$ in terms of depth, respectively, for $\omega_0 = 3$. As indicated in Fig. 7, the vertical displacement from $z = 0$ to $z = a$ should be equal to A as inferred from Eq. (1). Outside the disc, the displacement shows an oscillatory behavior as expected. As seen in Fig. 8, although the displacement is continuous at $z = 0$, its derivative with respect to depth is not continuous as indicated in (6) and illustrated in Figs. 5 and 6. As indicated in Figs. 5, 6 and 8, Both real and imaginary parts of the vertical displacement and vertical stress tend to zero with increasing depth. As frequency increases, both real and imaginary parts show oscillatory variation with the depth.

The oscillatory behavior of the response is clear from Figures 5 to 8. The wave number/wave length in the vertical and horizontal direction is a function of E' and G' , respectively. As G' is the same for all materials, the wave number is the same for all cases. However, there exist a clear difference between the wave number in vertical direction in the lower half-space, where the material changes from case to case.

The impedance/compliance function is a very important parameter in the subject of soil-structure-interaction. Because of this, the vertical impedance function is numerically evaluated in this study. Figs. 9, 10 and 11 show the real and imaginary parts of the vertical impedance function and compliance function obtained from the present study and the results of Luco and Mita (1987) and Pak and Gobert (1991) for four isotropic materials $\nu = 0.25, 1/3, 0.4$ and 0.45 for a high range of dimensionless frequency. in Figs. 9 and 10, the results of impedance function have been compared with the case of isotropic half-space for the Poisson's ratio $1/3$ and 0.45 . Also, in Figs. 11 the results of compliance function have been compared with the case of isotropic full-space for the Poisson's ratio 0.25 and 0.4 . As seen, there exists an excellent agreement between these two results, which shows the accuracy of the numerical evaluation in different steps. Finally, Fig.12 provide the vertical impedance function for different transversely isotropic bimetals at the interface ($z = 0$). As can be seen, the value of vertical impedance function for the case Mat I-Mat I is the highest since E'/E in material I is the largest. This can be seen an increase in the real part and the imaginary part.

7. CONCLUSIONS

In this paper, a mathematical analysis is presented for the vertical vibration of a massless rigid circular disc located at the interface of a transversely isotropic bi-material full-space. With the aid of Hankel transforms and a method of potentials, the mixed boundary-value problem is formulated as dual integral equations, which, in turn, are reduced to a Fredholm integral equation of the second kind. The Fredholm integral equation have been numerically solved. It is shown that the impedance functions are analytically in exact agreement with the existing solutions for a half-space with isotropic material properties. The impedance functions have been evaluated numerically, which can be used in the soil-structure-interaction problems.

Table 1. Synthetic material engineering constants.

Material	E (N/ mm ²)	E' (N/ mm ²)	G (N/ mm ²)	G' (N/ mm ²)	ν	ν'
I (Transversely isotropic)	50000	150000	20000	20000	0.25	0.25
II(Transverselyisotropic)	100000	50000	40000	20000	0.25	0.25
III(Transverselyisotropic)	150000	50000	60000	20000	0.25	0.25

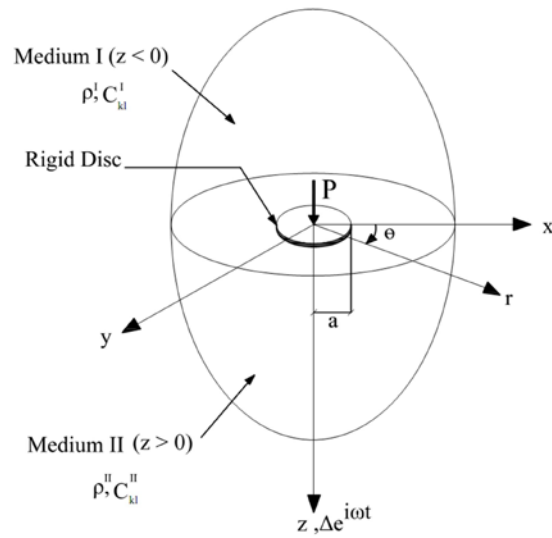


Figure 1. A rigid disc in a transversely isotropic bi-material full-space.

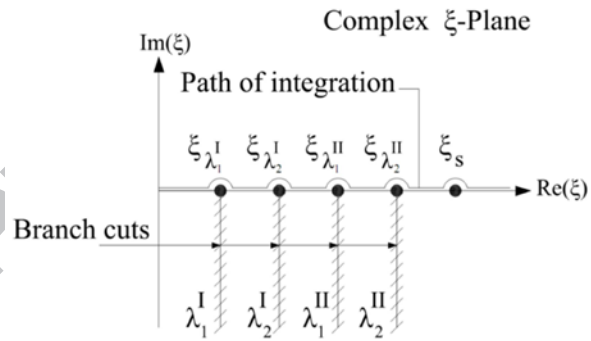


Figure 2. Path of integration for transversely isotropic bi-material full-space.

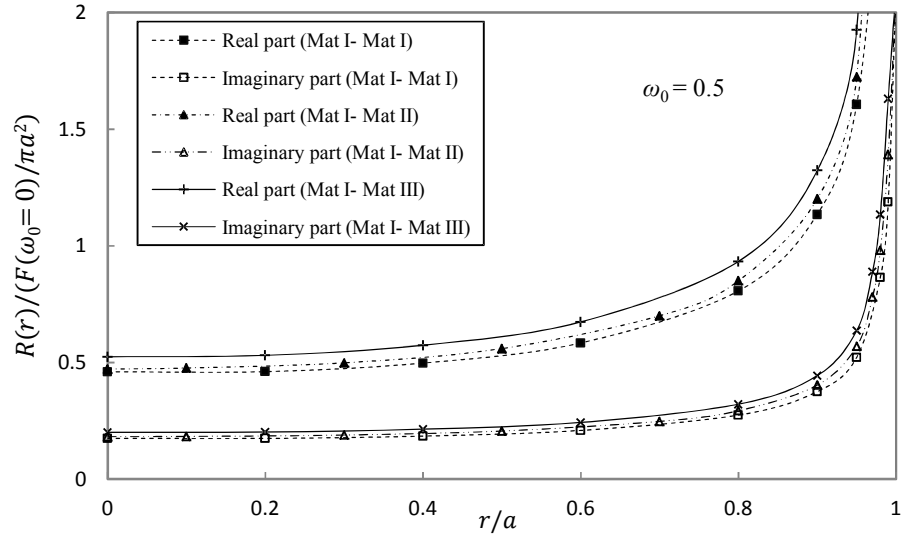


Figure 3. Normalized vertical stress for $\omega_0 = 0.5$ at $z=0$ in terms of horizontal distance for different transversely isotropic bimaterials.

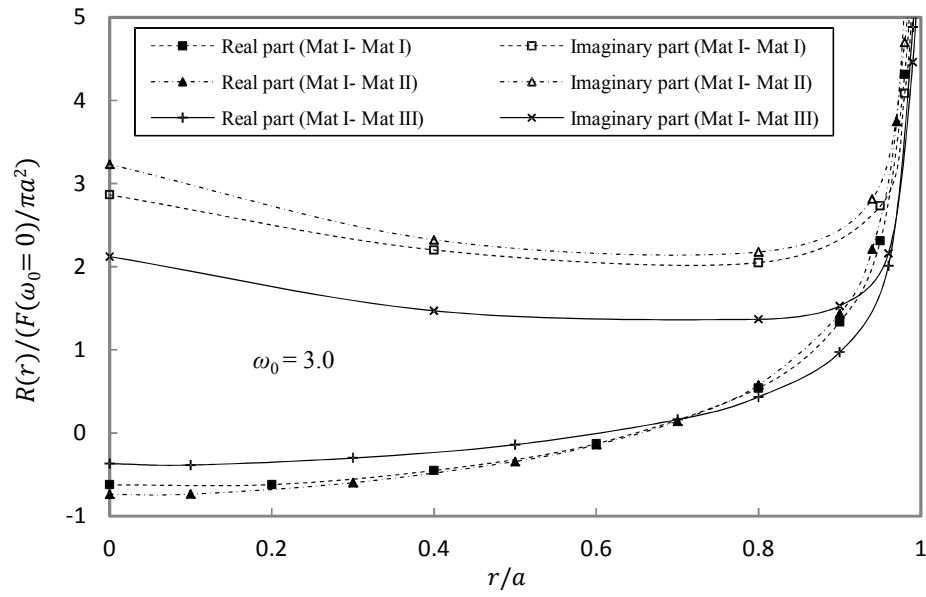


Figure 4. Normalized vertical stress for $\omega_0 = 3.0$ at $z=0$ in terms of horizontal distance for different transversely isotropic bimaterials.

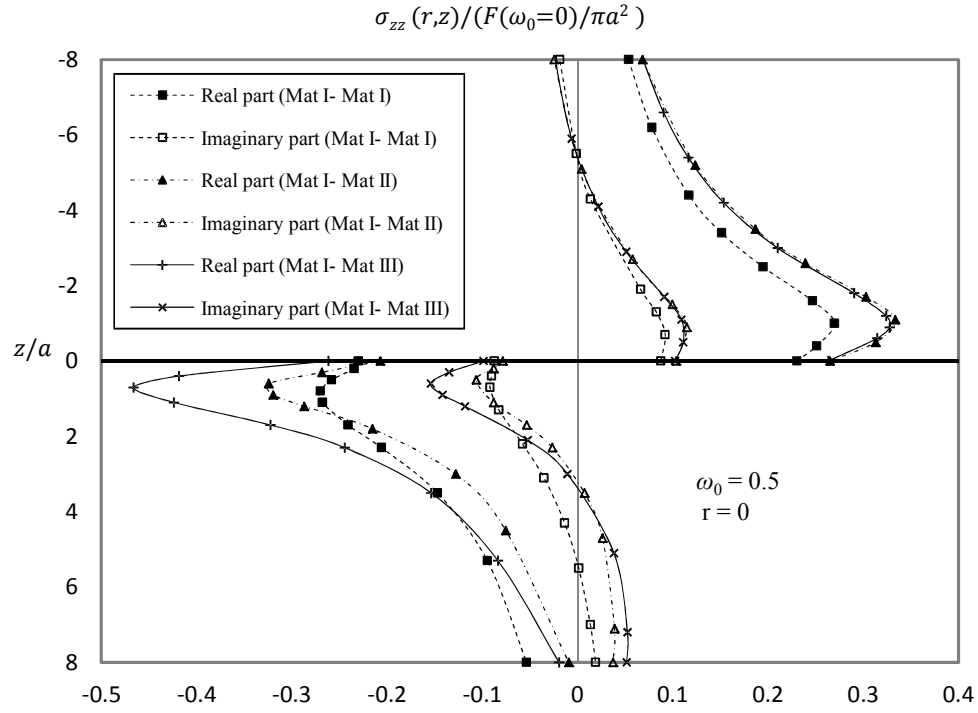


Figure 5. Normalized vertical stress for $\omega_0 = 0.5$ at $r = 0$ in terms of depth for different transversely isotropic bimetals.

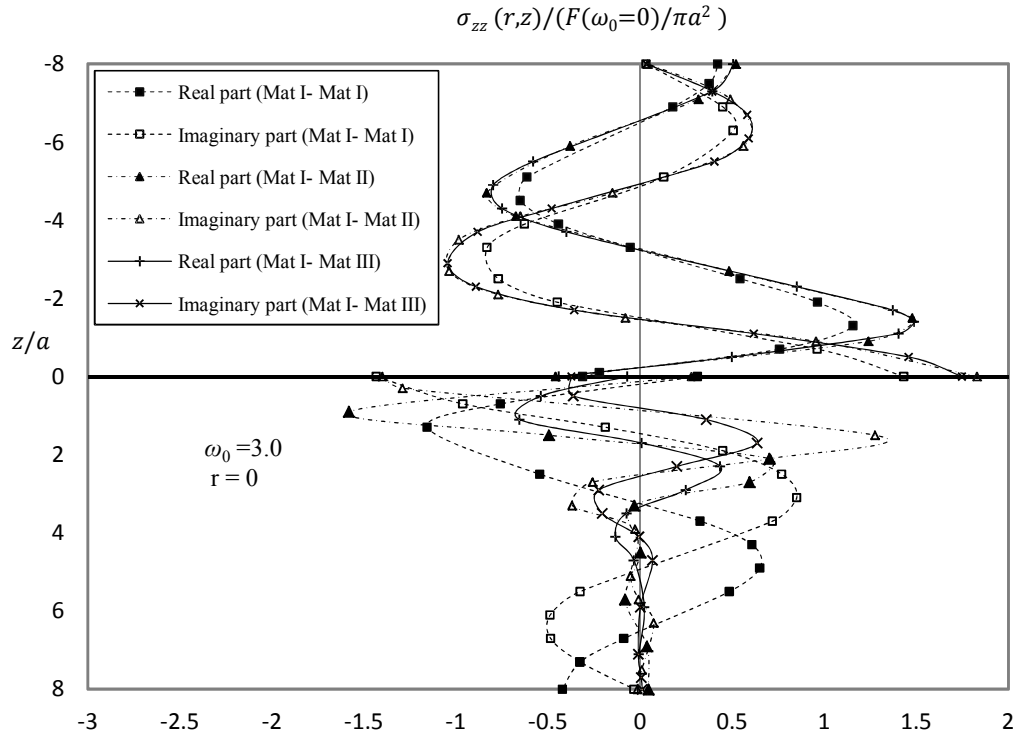


Figure 6. Normalized vertical stress for $\omega_0 = 3.0$ at $r = 0$ in terms of depth for different transversely isotropic bimetals.

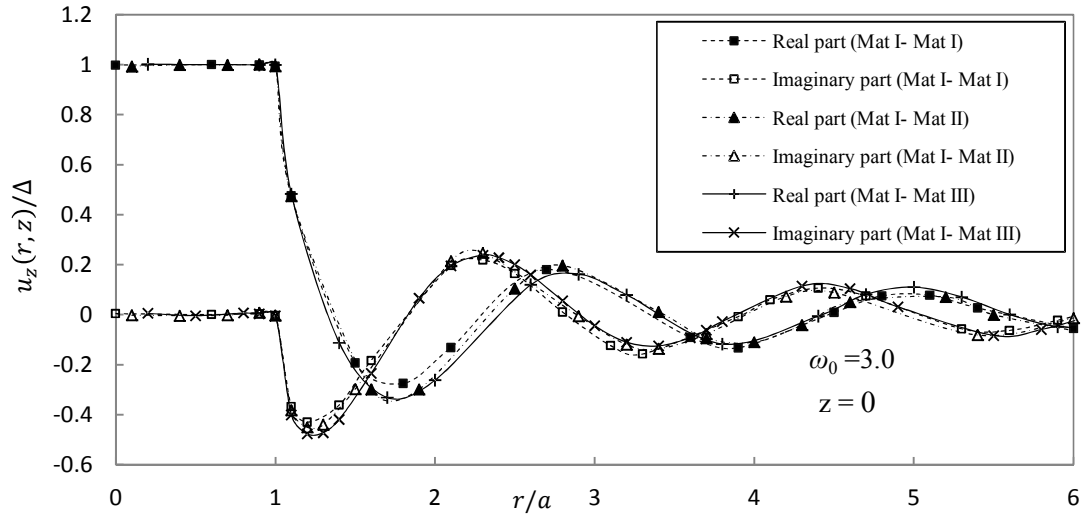


Figure 7. Normalized vertical displacement for $\omega_0 = 3.0$ at the interface in terms of the horizontal distance for different transversely isotropic bimaterials.

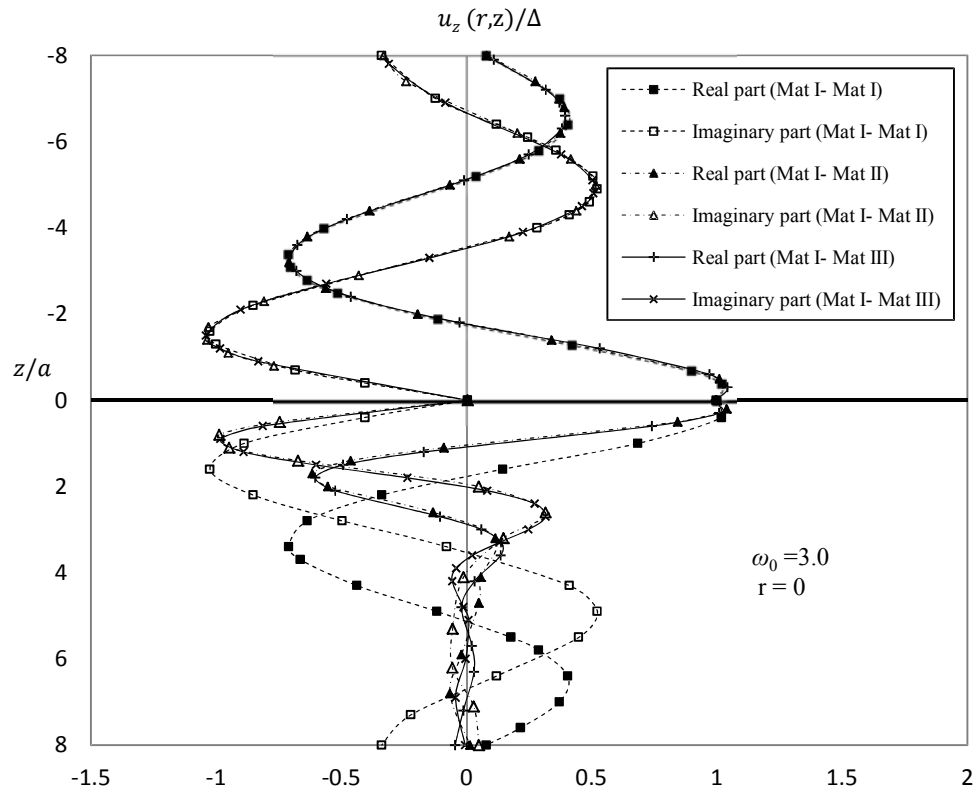


Figure 8. Normalized vertical displacement for $\omega_0 = 3.0$ at $r = 0$ in terms of depth for different transversely isotropic bimaterials.

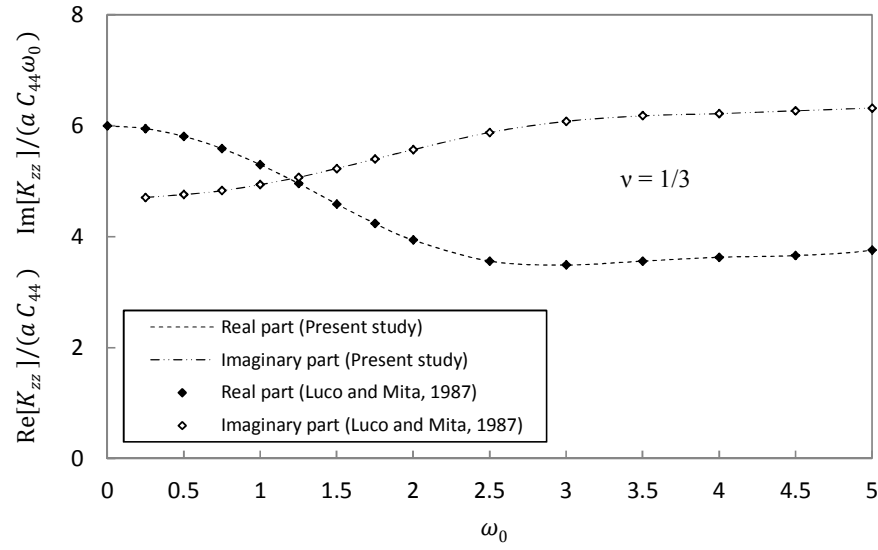


Fig. 9. Comparison of real and imaginary parts of vertical impedance function for isotropic material with $\nu = 1/3$.

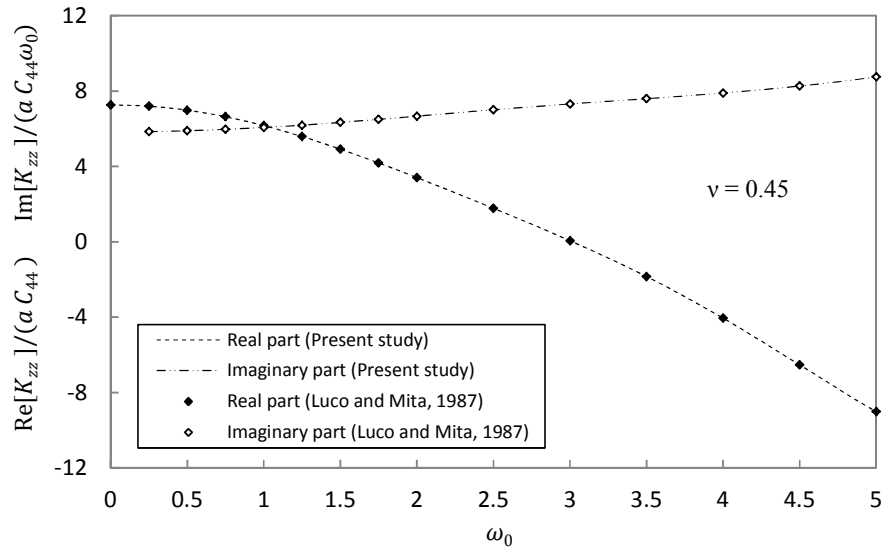


Fig. 10. Comparison of real and imaginary parts of vertical impedance function for isotropic material with $\nu = 0.45$.

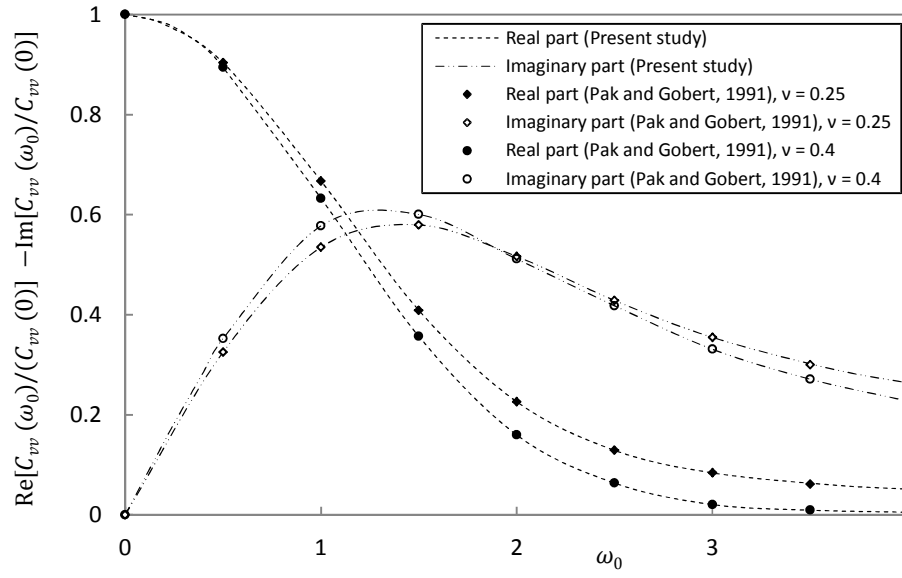


Figure 11. Comparison of real and imaginary parts of vertical compliance function for isotropic material with $\nu=0.25$ and $\nu=0.4$

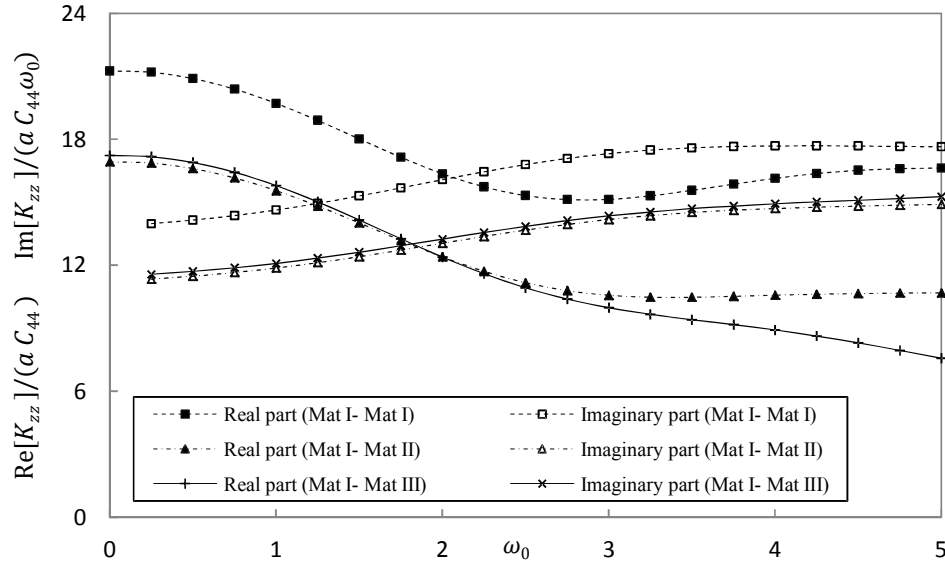


Figure 12. Real and imaginary parts of vertical impedance function for different transversely isotropic materials.

REFERENCES

- Apsel, R.J., Luco, J.E., 1983. On the Green's functions for a layered half space part II. *bssa*, 73(4): 931–951.
- Barnett, D.M., Lothe, J., Gavazza, S.D., Musgrave, M.J.P., 1985. Considerations of the existence of interfacial (Stoneley) waves in bonded anisotropic half-spaces. *rspl*, A 402: 153–166.
- Barnett, D.M., 2000. Bulk, surface, and interfacial waves in anisotropic linear elastic solids. *ijss*, 37: 45–54.
- Churchill, R.V., Brown, J.W., 1990. *Complex Variables and Applications*. McGraw-Hill, New York, NY.
- Destrade, M., Fu, Y.B., 2006. The speed of interfacial waves polarized in a symmetry plane. *ijes*, 44: 26–36.
- Eskandari-Ghadi M., 2005. A complete solutions of the wave equations for transversely isotropic media. *J Elasticity*, 81:1–19.
- Gladwell G.M.L., 1968. Forced tangential and rotatory vibration of a rigid circular disc on a semi-infinite solid. *ijes*, 6: 591–607.
- Katebi A.A., Khojasteh A., Rahimian M, Pak R.Y.S., 2010. Axisymmetric interaction of a rigid disc with a transversely isotropic half-space. *Int. J. Numer. Anal. Meth. Geomech*; 34, 1211–1236.
- Khojasteh A, Rahimian M, Pak R.Y.S., 2008. Three-dimensional dynamic Green's functions in transversely isotropic bi-materials. *ijss*, 45: 4952-4972.
- Kirkner David J., 1982. Vibration of a Rigid Disc on a transversely isotropic Elastic half-space. *Int. J. Numer. Anal. Meth. Geomech*, 6: 293-306.
- Lambros, J., Rosakis, A.J., 1995. Dynamic decohesion of bimaterials: experimental observations and failure criteria. *ijss*, 32 (17/18), 2677–2702.
- Lekhnitskii S.G., 1981. *Theory of anisotropic elastic bodies*. San Francisco, Calif: Holden-Day Publishing Co.
- Luco JE, Mita A., 1987. Response of a circular foundation on a uniform half-space to elastic waves. *Earthquake Eng Struct Dyn*, 15: 105–18.
- Mandal B.N, Mandal N., 1999. *Advances in dual integral equations*. CHAMPMAN & HALL/CRS.
- Moghaddasi H, Rahimian M, Khojasteh A, Pak R.Y.S., 2012. Asymmetric interaction of a rigid disc embedded in a transversely isotropic half-space. *qjmam*, DOI: 10.1093/hbs014.
- Noble B., 1963. The solution of Bessel function dual integral equations by a multiplying-factor method. *Proc Cambridge Phil Soc*, 59: 351–71.
- Pak, R.Y.S., Guzina, B.B., 2002. Three-dimensional Green's functions for a multi-layered half-space in displacement potentials. *ASCE*, 128(4): 449–461.
- Pak, RYS, Gobert A.T., 1991. Forced vertical vibration of rigid discs with an arbitrary embedment. *ASCE*, 117(11): 2527–48.
- Pak R.Y.S., Saphores J.D., 1991. Torsion of a rigid disc in a half-space. *ijes*, 29 (1): 1–12.

- Pak R.Y.S, Gobert A.T., 1990. On the axisymmetric interaction of a rigid disc with a semi-infinite solid. *ZAMP*, 41: 684–700.
- Payton RG., 1983. *Elastic Wave Propagation in Transversely Isotropic Media*. Martinus, Nijhoff: The Netherlands.
- Prasad, P.B.N., Hasebe, N., Wang, X.F., Shirai, Y., 2005. Green's functions for a bi-material problem with interfacial elliptical rigid inclusion and applications to crack and thin rigid line problems. *ijss*, 42: 1513–1535.
- Rahimian M, Eskandari-Ghadi M, Pak R.Y.S, Khojasteh A. 2007. An elastodynamic potential method for a transversely isotropic solid. *ASCE*, 133(10): 1134–45.
- Rahman M., 2001. The normal shift of a rigid elliptical disc in a transversely isotropic solid. *ijss*, 38: 3965-3977.
- Rajapakse R.K.N.D., Wang Y., 1993. Green's functions for transversely isotropic elastic half space. *ASCE*, 119(9): 1724–1746.
- Reissner E, Sagoci H.F., 1944. Forced torsional oscillations of an elastic half-space. *jap.aip*, 15(9): 652–4.
- Robertson I.A., 1966. Forced vertical vibration of a rigid circular disc on a semi-infinite elastic solid. *Proc Cambridge Phil Soc*, 62(A): 547–53.
- Selvadurai, A.P.S., 1994. Analytical methods for embedded flat anchor problems in geomechanics. *Proc. 8th Int. Conf. Int. Assoc. Comp. Meth. Adv. Geomech*, vol. 1. 305–321.
- Selvadurai, A.P.S., 2000. An inclusion at a bi-material elastic interface. *J. Engng. Math.* 37, 155–170.
- Selvadurai, A.P.S., 2003. On certain bounds for the in-plane translational stiffness of a disc inclusion at a bi-material elastic interface. *mechrescom*, 30: 227–234.
- Shahmohamadi M, Khojasteh A, Rahimian M, Pak R.Y.S., 2011a. Seismic response of an embedded pile in a transversely isotropic half-space under incident P-wave excitations. *soildyn*, 31(3): 361-371.
- Shahmohamadi M, Khojasteh A, Rahimian M, Pak R.Y.S., 2011b. Axial soil–pile interaction in a transversely isotropic half-space. *ijes*, 49(9): 934-949.
- Shahmohamadi M, Khojasteh A, Rahimian M, Pak R.Y.S., 2012. Rigid cylinder in a transversely isotropic half-space under lateral loads. *Int. J. Numer. Anal. Meth. Geomech*, 36(19): 1368-1386.
- Sneddon I.N., 1966. *Mixed boundary value problems in potential theory*. Amsterdam: North-Holland Publishing Company.
- Wu, X.F., Dzenis, Y.A., Fan, T.Y., 2003. Two semi-infinite interfacial cracks between two bonded dissimilar elastic strips. *ijes*, 41: 1699–1710.
- Zeng X. and Rajapakse R.K.N.D., 1999. Vertical Vibrations of a Rigid Disc Embedded in a Poroelastic Medium. *Int. J. Numer. Anal. Meth. Geomech*, 23: 2075-2095.